Cellular and Molecular Life Sciences (2023) 80:10
https://doi.org/10.1007/s00018-022-04649-9

ORIGINAL ARTICLE

Deleting interleukin-10 from myeloid cells exacerbates atherosclerosis in *Apoe*$^{-/-}$ mice

Marco Orecchioni[1] · Dennis Wolf[2] · Vasantika Suryawanshi[1] · Holger Winkels[3] · Kouji Kobiyama[4] · Jeffrey Makings[1] · William B. Kiosses[5] · Klaus Ley[1,6,7]

Received: 6 May 2022 / Revised: 5 November 2022 / Accepted: 23 November 2022 / Published online: 10 December 2022
© The Author(s), under exclusive licence to Springer Nature Switzerland AG 2022

Abstract

Atherosclerosis is initiated by subendothelial retention of lipoproteins and cholesterol, which triggers a non-resolving inflammatory process that over time leads to plaque progression in the artery wall. Myeloid cells and in particular macrophages are the primary drivers of the inflammatory response and plaque formation. Several immune cells including macrophages, T cells and B cells secrete the anti-inflammatory cytokine IL-10, known to be essential for the atherosclerosis protection. The cellular source of IL-10 in natural atherosclerosis progression is unknown. This study aimed to determine the main IL10-producing cell type in atherosclerosis. To do so, we crossed VertX mice, in which IRES-green fluorescent protein (eGFP) was placed downstream of exon 5 of the *Il10* gene, with atherosclerosis-prone *Apoe*$^{-/-}$ mice. We found that myeloid cells express high levels of IL-10 in VertX *Apoe*$^{-/-}$ mice in both chow and western-diet fed mice. By single cell RNA sequencing and flow cytometry analysis, we identified resident and inflammatory macrophages in atherosclerotic plaques as the main IL-10 producers. To address whether IL-10 secreted by myeloid cells is essential for the protection, we utilized *LyzM*$^{Cre+}$*Il10*$^{fl/fl}$ mice crossed into the *Apoe*$^{-/-}$ background and confirmed that macrophages were unable to secrete IL-10. Chow and western diet-fed *LyzM*$^{Cre+}$*Il10*$^{fl/fl}$ *Apoe*$^{-/-}$ mice developed significantly larger atherosclerotic plaques as measured by *en face* morphometry than *LyzM*$^{Cre-}$*Il10*$^{fl/fl}$*Apoe*$^{-/-}$. Flow cytometry and cytokine measurements suggest that the depletion of IL-10 in myeloid cells increases Th17 cells with elevated CCL2, and TNFα in blood plasma. We conclude that macrophage-derived IL-10 is critical for limiting atherosclerosis in mice.

Keywords Atherosclerosis · Immune cells · Inflammation · Macrophages · Cytokines

Background

Atherosclerosis and its sequelae stroke, myocardial infarction and ischemic heart failure are the leading cause of mortality in USA and worldwide [1]. Atherosclerosis is initiated by excess lipoproteins and cholesterol, which triggers a chronic inflammatory process that over time drives plaque progression in the artery wall [2].

Myeloid cells and in particular macrophages are the primary drivers of the initial inflammatory response and

✉ Marco Orecchioni
morecchioni@lji.org

✉ Klaus Ley
KLEY@augusta.edu

1 La Jolla Institute for Immunology, 9420 Athena Circle Drive, La Jolla, CA 92037, USA

2 Cardiology and Angiology I, Medical Center–University of Freiburg, Faculty of Medicine, University of Freiburg, Freiburg, Germany

3 Department of Cardiology, Faculty of Medicine and University Hospital Cologne, University of Cologne, Cologne, Germany

4 Division of Vaccine Science, Department of Microbiology and Immunology, The Institute of Medical Science, The University of Tokyo, Tokyo, Japan

5 Histology and Microscopy Core Facility, La Jolla Institute for Immunology, La Jolla, CA 92037, USA

6 Department of Bioengineering, University of California San Diego, La Jolla, CA 92093, USA

7 Immunology Center of Georgia (IMMCG), Augusta University, Augusta, GA 30912, USA

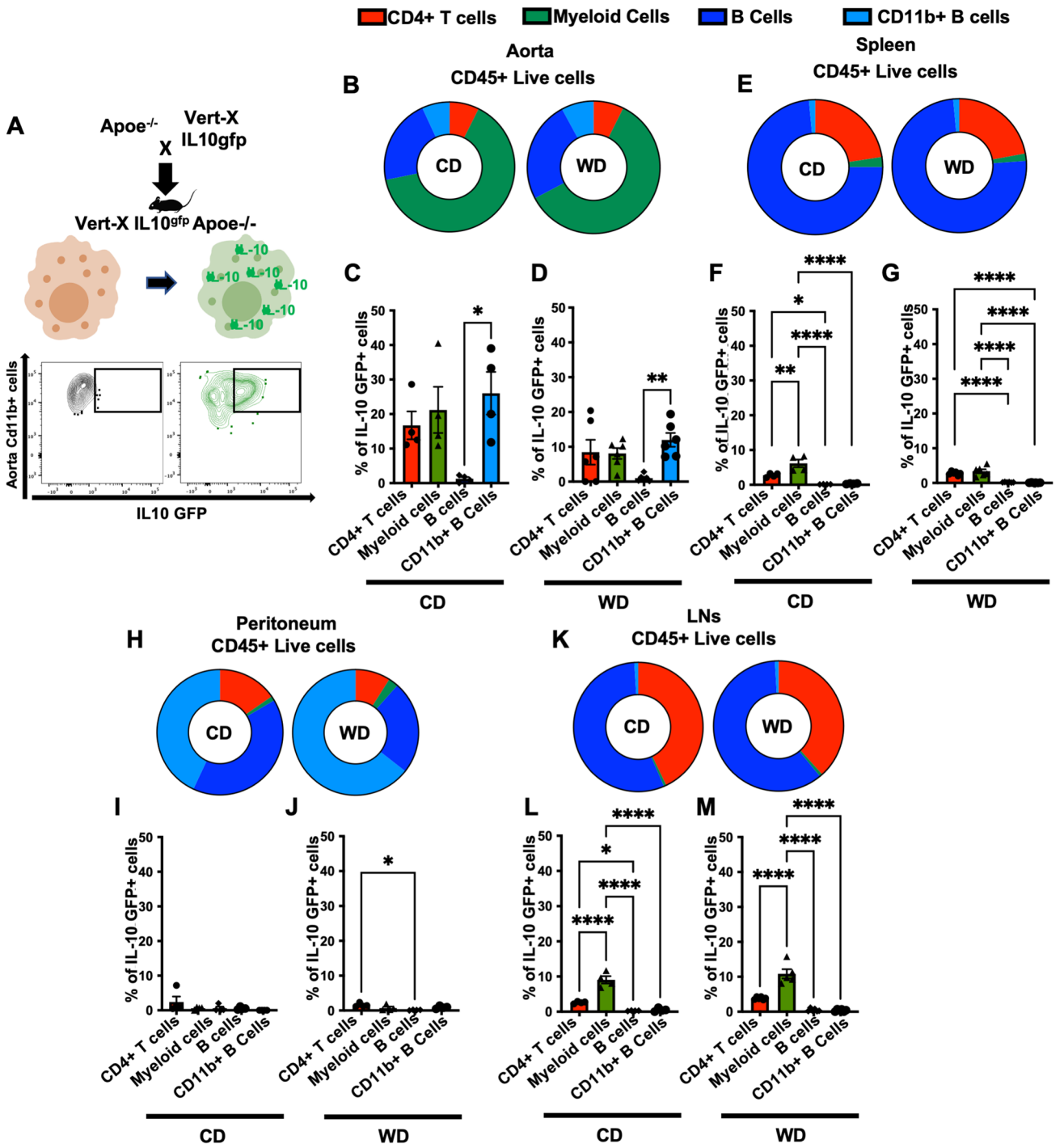

atherosclerotic plaque formation [2]. During hyperlipidemic conditions, there is a rapid recruitment of circulating monocytes into the atherosclerosis-prone areas of the arterial intima which then differentiate to macrophages and take up atherogenic cholesterol ester-rich lipoprotein becoming foam cells [3]. Plaque macrophages can have pro-inflammatory or anti-inflammatory features. Recent single cell studies by mass cytometry and single cell RNA sequencing (scRNA-seq) have defined at least five distinct subsets of macrophages in mouse aortas: resident, inflammatory, Trem2$^+$ foamy, cavity and IFNIC macrophages [4]. Cell surface protein markers are not fully defined for most of these subsets; however, CD206 and Lyve1 have been proposed as good markers to discriminate resident macrophages [4, 5]. Macrophages are an important source of cytokines in the lesion and can secrete several proinflammatory cytokines such as (Interleukin) IL-1, IL-6, IL-12, IL-15, IL-18 as well as anti-inflammatory cytokines such as IL-10 [6].

◂**Fig. 1** IL-10 expression in mouse tissue leukocytes **A** VertX mice, in which an IRES-enhanced green fluorescent protein (eGFP) fusion protein was placed downstream of exon 5 of the IL-10 gene, were crossed into the atherosclerosis-prone *Apoe*$^{-/-}$ background. **B** Aortic leukocyte composition as % of live CD45^{+} cells in aortas of VertX *Apoe*$^{-/-}$ mice fed WD, (8 weeks, $n=6$) or CD (16 weeks, $n=4$). **C** IL-10^{GFP+} expression reported as % of parent cell type from aortas of VertX *Apoe*$^{-/-}$ mice on CD (16 weeks). **D** IL-10^{GFP+} expression reported as % of parent cell type from aortas of VertX *Apoe*$^{-/-}$ mice on WD (8 weeks). **E** Spleen leukocyte composition expressed as % of total CD45^{+} live cells from VertX *Apoe*$^{-/-}$ mice on WD (8 weeks, $n=6$) or kept on CD (16 weeks, $n=4$). **F** IL-10^{GFP+} expression reported as % of parent cell type of IL-10^{GFP+} from spleen of Vert-X *Apoe*$^{-/-}$ mice on CD. **G** IL-10^{GFP+} expression reported as % of parent cell type from spleen of VertX *Apoe*$^{-/-}$ mice on WD. **H** Leukocyte composition expressed as % of total CD45^{+}, Live cells in peritoneal lavage fluid of Vert-X *Apoe*$^{-/-}$ mice challenged with a WD (8 weeks, $n=5$) or kept in CD (16 weeks, $n=5$). **I)** IL-10^{GFP+} expression reported as % of parent cell type from peritoneal lavage fluid of VertX *Apoe*$^{-/-}$ mice on CD. **J** IL-10^{GFP+} expression reported as % of parent cell type from peritoneal lavage fluid of VertX *Apoe*$^{-/-}$ mice on WD. **K** Leukocyte composition expressed as % of total CD45^{+}, live cells in draining LNs of Vert-X *Apoe*$^{-/-}$ mice challenged with a WD (8 weeks, $n=5$) or kept on CD. **L** IL-10^{GFP+} expression reported as % of parent cell type from LNs of VertX *Apoe*$^{-/-}$ mice on CD. **M** IL-10^{GFP+} expression reported as % of parent cell type of IL-10^{GFP+} from LNs of VertX *Apoe*$^{-/-}$ mice on WD. Representative gating scheme in S.Fig. 1. Data are presented as mean ± SEM. *P* value was calculated by one-way ANNOVA test with Tukey's correction for multiple comparison $*p<0.05$, $**p<0.01$, $***p<0.001$, $****p<0.0001$

IL-10 is a prototypic anti-inflammatory cytokine produced by several immune cells such as macrophages, T cells and B cells [7]. IL-10 signals via of a two-subunit receptor composed of IL-10 receptor (IL-10R)1 and 2 [8]. IL-10R2 is constitutively expressed by most cells, whereas IL-10R1 is mostly restricted to the hematopoietic lineage [8–10]. After binding to its receptor, IL-10 activates the canonical Janus kinase (JAK)/signal transducer and activator of transcription (STAT) pathway, specifically JAK1 and STAT3, which subsequently induces the expression of genes associated with anti-inflammatory and immunosuppressive functions [11].

IL-10 expression has been shown to be essential to protect against atherosclerosis [12] in both *Ldlr*$^{-/-}$ [13–15] and *Apoe*$^{-/-}$ [16] models of atherosclerosis. Mallat and colleagues showed that atherosclerotic lesions of IL-10-deficient mice had increased T-cell infiltration, increased macrophages content and decreased collagen content [12]. This was confirmed by the same group in *Ldlr*$^{-/-}$ mice transferred with *Il10*-deficient bone marrow [15]. Pinderski et al. also showed similar results in *Ldlr*$^{-/-}$ mice, and they also suggested that the inhibition was mediated by a specific shift toward a Th2 phenotype with subsequent alteration in monocyte and lymphocyte function [17]. Caligiuri et al. assessed the effect of IL-10 deficiency in *Apoe*$^{-/-}$ model [16]. They found changes in cholesterol composition and increased lesion size in the *Il10*$^{-/-}$ *Apoe*$^{-/-}$ mice after 16 weeks of western diet (42% of calories from fat) [16]. Finally, Han and colleagues found that overexpressing IL-10 in macrophages reduced atherosclerosis in *Ldlr*$^{-/-}$ mice. They suggested that macrophage-derived IL-10 may decrease foam cell apoptosis, which would be an autocrine effect [18]. However, a recent report showed that loss of myeloid IL-10R1 unexpectedly attenuated atherosclerotic lesion size [19], possibly ruling out a beneficial effect of autocrine IL-10 on myeloid cells.

Here, we use a loss-of-function approach to identify the relevant IL-10-producing cells in atherosclerosis. First, we crossed IL-10 VertX reporter mice [20] with *Apoe*$^{-/-}$ mice. In VertX mice, the GFP expression strictly correlates to the IL-10 expression and IL-10 protein levels, as shown by gene expression analysis and ELIspot. GFP intensity is, however, reported to be retained longer than the actual IL-10 protein in the cells [20]. Using this model, we find that most of the IL-10 in the atherosclerotic aorta is derived from CD11b^{+} myeloid cells, which are mostly macrophages. We identified that Lyve-1^{+} CD206^{+} resident macrophages produced high levels of IL-10. A smaller proportion of non-resident CD206^{-} Lyve1^{-} macrophages also expressed IL-10. Next, to determine the relevance of myeloid-derived IL-10 in the progression of atherosclerosis, we crossed *LyzM*$^{Cre+}$ [21] *Il10*$^{fl/fl}$ [22] mice into the *Apoe*$^{-/-}$ background and observed significantly increased atherosclerotic lesion size in mice fed chow diet (CD), representing a slower model with moderate cholesterol elevation [23]. We also tested western-type diet (WD) fed *Apoe*$^{-/-}$ mice, which represents an accelerated atherosclerosis model [23].

Methods

Mice

Vert-X, *Apoe*$^{-/-}$, *LyzM*$^{Cre+}$ (Lyz2tm1(cre)Ifo/J), and *Il10*$^{fl/fl}$ mice on a C57BL/6J background were purchased from Jackson Laboratories crossed and maintained in-house on a 12 h light/dark cycle. For atherosclerosis studies, 8-week-old male *LyzM*$^{Cre+}$ *Il10*$^{fl/fl}$ *Apoe*$^{-/-}$ and *LyzM*$^{Cre-}$*Il10*$^{fl/fl}$*Apoe*$^{-/-}$ mice were fed a standard chow diet (CD) until 16/25 weeks of age or a western-type diet (WD) containing 43% calories from fat and 0.2% cholesterol (Envigo, TD.88137) for 8/12 weeks. *LyzM*$^{Cre+}$ *Il10*$^{fl/fl}$ *Apoe*$^{-/-}$ showed 10–20% incidence of inflammatory bowel diseases displayed by anus prolapses. Any sign of anus prolapse was considered as exclusion criteria from the present study. Thus, all the mice considered and analyzed in the experiments reported were not showing any signs of inflammatory bowel diseases.

Mice were euthanized by CO_2 inhalation. Mouse whole blood was collected in EDTA tubes via cardiac puncture. Blood leukocyte counts were determined by HemaVet

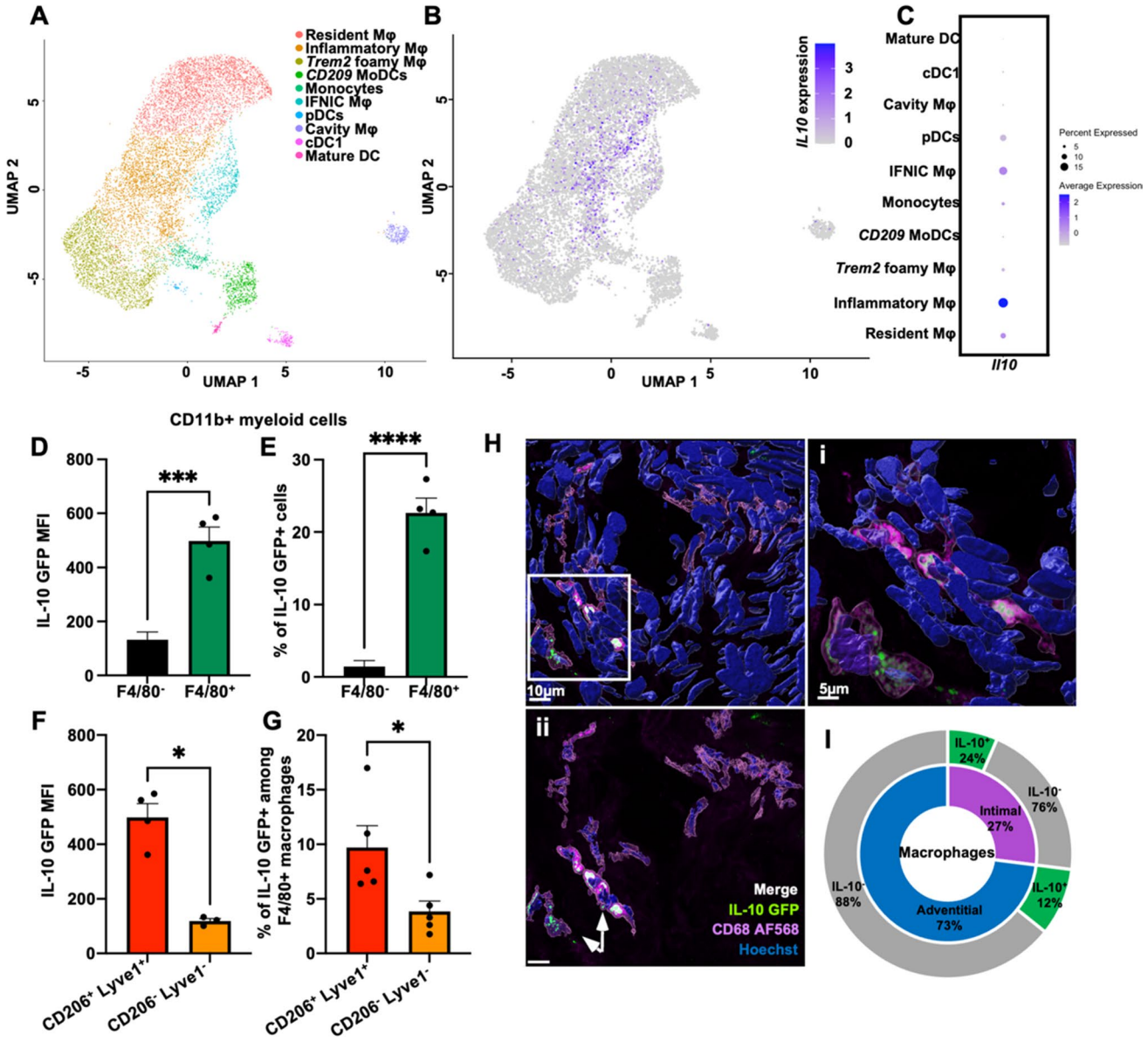

Fig. 2 IL-10 expression in vascular macrophages. **A** The Uniform Manifold Approximation and Projection (UMAP) clustering of myeloid cells (macrophages, mixed monocyte/macrophage/dendritic cell (DC) clusters) as in [4]. **B** Single cell *Il10* expression plotted on myeloid cell clusters. **C** Heatmap showing the levels of *Il10* expression in all the myeloid clusters retrieved. **D**, **E** IL-10 expression in $CD45^+$ live $TCR\beta^-$ $CD19^-$ $F4/80^+$ vascular macrophages from VertX $Apoe^{-/-}$ aortae, reported as (**D**) MFI and (**E**) % relative to parent population ($n = 4$–5). $Apoe^{-/-}$ aortae were used as controls. **F**, **G** Flow cytometric analysis of IL-10 expression in $CD45^+$, live, $TCR\beta^-$, $CD19^-$, $F4/80^+$, $CD206^+$ $Lyve1^+$ resident, and $CD206^-$ $Lyve1^-$ non-resident vascular macrophages from VertX $Apoe^{-/-}$ aortae, reported as (**F**) MFI and (**G**) % relative to parent population ($n = 4$–5). MFI and % data shown have been subtracted to $GFP^-Apoe^{-/-}$ control. **H** Confocal fluorescence micrographs depicting IL-10 (green), CD68 (magenta) immunoreactivity, and Hoechst (blue) nuclear staining in whole mount aorta from a VertX $Apoe^{-/-}$ mouse fed WD. (i) Increased magnification showing $IL\text{-}10^{GFP+}$ (green) and $CD68^+$ (magenta) macrophages. Scale bars 5 μm. (ii) Micrograph showing only $CD68^+$ macrophages detected in the imaged field. Scale bars 10 μm. Co-localized green and magenta signal appears white and identify $IL\text{-}10^{GFP+}$ macrophages. **I** Quantification of intimal and adventitial macrophages expressing IL-10 as identified by confocal microscopy. Data are presented as mean ± SEM. *P* value was calculated by unpaired *T* test with Welch's correction $*p < 0.05$, $***p < 0.001$, $****p < 0.0001$

950 (Drew Scientific). Plasma was collected from EDTA-blood centrifuged at 2500×*g* for 15 min at 4 °C and stored at − 80 °C until further analysis.

Aorta collection and processing

Aortas were harvested and digested as previously described [24]. For flow cytometry analysis, surgically excised aortas

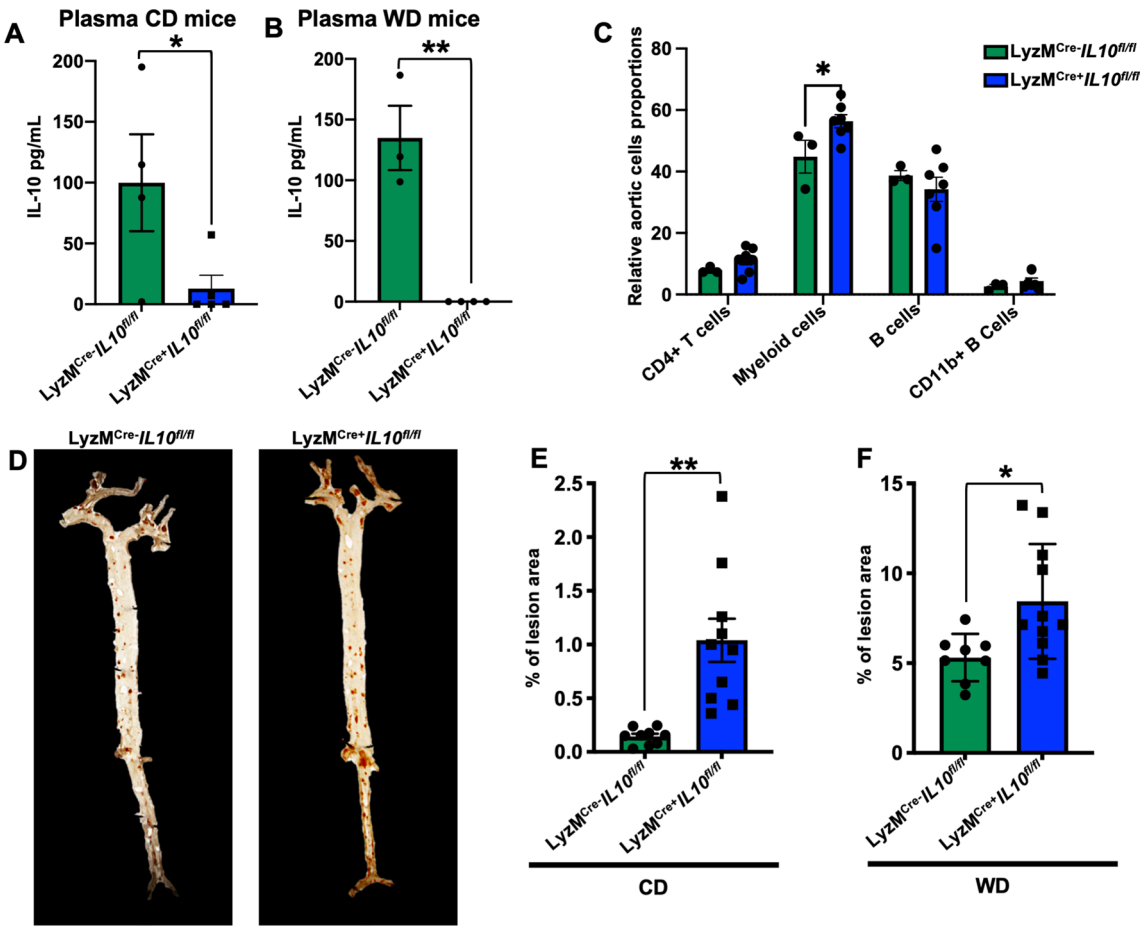

Fig. 3 IL-10 deletion in myeloid cells exacerbates atherosclerosis. IL-10 levels measured by CBA in plasma of *LyzM*$^{Cre+}$*Il10*$^{fl/fl}$ *Apoe*$^{-/-}$, or *LyzM*$^{Cre-}$*Il10*$^{fl/fl}$ *Apoe*$^{-/-}$ mice fed **A** CD for 25 weeks or **B** WD for 12 weeks. **C** Aortic immune cells relative proportion (%) in *LyzM*$^{Cre+}$*Il10*$^{fl/fl}$ *Apoe*$^{-/-}$, or *LyzM*$^{Cre-}$*Il10*$^{fl/fl}$ *Apoe*$^{-/-}$ mice fed CD. **D** Pictures reporting en-face atherosclerosis evaluation in aortas harvested from atherosclerosis prone *LyzM*$^{Cre+}$*Il10*$^{fl/fl}$ *Apoe*$^{-/-}$, or *LyzM*$^{Cre-}$*Il10*$^{fl/fl}$ *Apoe*.$^{-/-}$ mice and formally quantified after 25 weeks of age fed in (**E**) CD ($n=10$) or (**F**) after 12 weeks of WD ($n=8/11$). Data are presented as mean ± SEM. *P* value was calculated by two-way ANOVA and unpaired T test with Welch's correction. $^{*}p<0.05$, $^{**}p<0.01$

were collected in 1 mL RPMI media (Gibco) containing 10% fetal bovine serum (FBS) on ice. Aortas were then cut into small pieces and individually digested for 1 h at 37 °C in HBSS (with Ca^{2+} and Mg^{2+}) containing 450 U/mL Collagenase I (Sigma Aldrich), 250 U/mL Collagenase XI (Sigma Aldrich), 120 U/mL Hyaluronidase (Sigma Aldrich), and 120 U/mL DNase I (Worthington). The digested aortic suspension was subsequently filtered through a 50 µm cell strainer (Partec) and washed with 37 °C pre-warmed RPMI 1640 containing 10% FBS and 1% Pen/Strep solution from now on called complete media (5 min, 500×g). Cells were kept in complete media for 30 min at 37 °C in a cell culture incubator to allow for the recovery of cell surface molecule expression affected by digestion.

Lymph node (LNs) cells, splenocytes isolation, and peritoneal lavage

LNs cells and splenocytes were isolated by meshing LNs (cervical, axillary, brachial, inguinal and mesenteric) and spleens through a 70 µm cell strainer (BD Biosciences). Splenocytes were then washed with PBS, followed by red blood cell lysis for 10 min (eBioscience). All cells were washed two times in PBS, and the cell concentration was adjusted to 1×10^{6}/mL in PBS. Peritoneal cells were collected by lavage of the peritoneal cavity. Briefly, the peritoneal cavity of mice was injected with 5 mL of ice-cold PBS and massaged gently to dislodge any loosely attached cells. Then, peritoneal fluid was extracted and washed twice with PBS by centrifugation at 500×*g* for 5 min at 4 °C. Cells were then resuspended in 4 °C cold PBS.

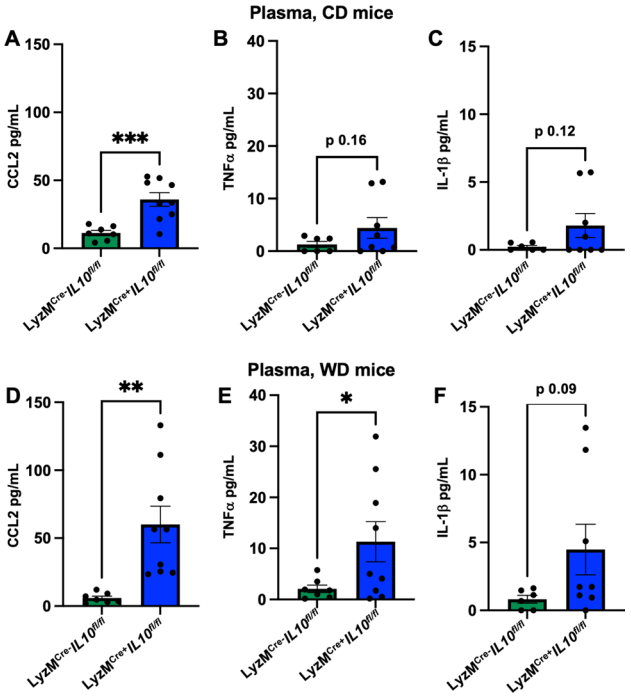

Fig. 4 Myeloid IL-10 deletion elevates systemic cytokines and chemokines in $LyzM^{Cre+}Il10^{fl/fl}$ $Apoe^{-/-}$ mice. CCL2, TNFα and IL-1β assessed by CBA in plasma of $LyzM^{Cre+}Il10^{fl/fl}$ $Apoe^{-/-}$ fed CD or WD. **A**–**C** Histogram showing modulated levels for CCL2, TNFα and IL-1β in plasma of $LyzM^{Cre+}Il10^{fl/fl}$ $Apoe^{-/-}$ fed (**A**–**C**) CD and (**D**–**F**) WD. Data are presented as mean ± SEM. *P* value was calculated by unpaired *T* test with Welch's correction. $^{*}p < 0.05$, $^{**}p < 0.01$. $^{***}p < 0.001$

Flow cytometry analysis

LNs, splenic and aortic cells were stained in the dark for 20 min at RT with a mixture of anti-mouse CD45-PerCP (clone 30-F11, Biolegend), CD11b-PE-Cy7 (clone M1/70, Biolegend), TCRβ-BV711 (clone H57-597, Biolegend), CD4-PE-AlexaFluor610 (clone GK1.5, Invitrogen), CD19-APC-Cy7 (clone 6D5, Biolegend), Ly6G-BV786 (clone RB6-8C5, BD Biosciences), F4/80-BV421 (clone BM8, Biolegend), CD206-BV650 (clone C068C2, Biolegend) and Lyve1-PE (clone ALY7, Biolegend) antibodies and the live/dead (LD) Yellow or LD FVS700 fixable dye (cat# 564997, BD Biosciences).

For intracellular staining, LNs, splenic and aortic cells were stimulated for 4 h with 1X Cell Stimulation Cocktail (cat# 00-4970-93, eBioscience) and 1X Protein Transport Inhibitor Cocktail (cat# 00-4980-03 eBioscience) according to the manufacturer's instructions. After incubation, cells were washed thrice and fixed with 2% paraformaldehyde (PFA) for 20 min. Cells were washed, resuspended in 1x permeabilization buffer (cat# 00-8333-56, eBioscience), centrifuged for 5 min, 500×*g* and incubated with a mixture of anti-mouse TNF-PE (clone MP6-XT22, Biolegend) and IL-10-APC (clone JES5-16E3, Biolegend) in 1x permeabilization buffer at 4 °C for 30 min. Cells were washed, resuspended in PBS containing 2% FBS, and acquired on a LSRII flow cytometer (BD Biosciences).

For intranuclear staining, LNs cells were treated following the eBioscience FOXP3 transcription factor staining protocol (cat # 00-5523-00). LNs cells were incubated for 20 min in the dark with a mixture of surface markers: anti-mouse CD45-PerCP (clone 30-F11, Biolegend), TCRβ-AF700 (clone H57-597, Biolegend), CD4-APCef780 (clone GK1.5, Invitrogen), CD44-BV650, (clone IM7, Biolegend), CD62L-BV570 (clone MEL-14, Biolegend) and for 30 min in the dark with intranuclear markers: Foxp3-FITC (clone FJK-16s, eBioscience), T-bet-BV421, (clone 4B10, Biolegend), RORyt-PE-CF594 (clone Q31-378, BD Biosciences), GATA3-BV711 (clone L50-823, BD Biosciences), and BCL6-PECy7 (clone K112-91, BD Biosciences). After incubation cells were washed, resuspended in PBS containing 2% FBS, and acquired on a LSRII flow cytometer (BD Biosciences).

Whole mount imaging

Aortae from *Vert-X* $Apoe^{-/-}$ and $Apoe^{-/-}$ mice were carefully cleaned in situ and fixed in 2% PFA at 4 °C for 24 h, washed with PBS and transferred to 5 mL incubation buffer [2% FBS, 0.5% saponin (cat#47036, Sigma Aldrich), 0.1% sodium azide (cat# S2002, Sigma Aldrich)] containing CD68 primary antibody (1:200 cat# ab125212, Abcam), and anti-GFP AF488 (1:100 clone FM264G, Biolegend) and agitated for 24 h at 37 °C. Aortas were then washed 5 times with PBS and stained in 5 mL incubation buffer containing secondary anti-rabbit IgG-AF598 (1:500, cat# A32740 Thermo Fisher), and Hoechst (1:10,000) for 24 h at 37 °C with agitation. Stained aortas were washed with PBS, opened longitudinally, mounted between glass slides, and imaged from the adventitial side with a Zeiss LSM880 confocal scanning microscope. Image acquisition settings were set with control samples (wt samples, and secondary anti-rabbit IgG-AF598 control) and maintained throughout the experiment. Image and scan processing were performed with Zen microscope software (Zeiss) and Imaris analysis software (Bitplane).

En face lesion quantification

Mice were sacrificed, perfused with PBS supplemented with 2% heparin (cat# C504710, Fresenius Kabi USA, LLC), aortas were dissected for en face staining. After explant, each aorta was incubated with 4% PFA for at least 24 h at 4 °C and pinned out. Atherosclerotic plaques were stained

by Sudan IV. Atherosclerotic lesion size measurement was performed by blinded investigators using Image-Pro Premier software (Media Cybernetics) or Qpath (v0.2.3) [25]. Aortas with insufficient quality (extensive tissue damage) were excluded from further analysis. Possible outliers were assessed by ROUT test with $Q = 1\%$.

Plasma lipid analysis

Plasma from experimental mice was tested for lipid content by IDEXX BioResearch (6290-Lipid Panel Rodent).

Cytokine bead array

Plasma samples harvested as above described were analyzed by BD CBA Flex Sets (BD Biosciences) for mouse IL-10 (cat# 558300), IL-1β (cat# 560232), TNFα (cat# 558299) and CCL2 (MCP1 cat# 558342).

scRNA-seq meta data

The RNA single cell meta-data reported in this manuscript are based on previously reported data [4]. Briefly, scRNA-Seq data from 9 datasets were analyzed using the latest bioinformatics integration method Harmony [26]. Cells were visualized using the Uniform Manifold Approximation and Projection [27], and colored based on *Il10* expression.

Statistics

For visualization and statistical testing of normally distributed, continuous variables between two groups, an unpaired, two-sided Student's *T* test with Welch correction was applied. Significances between multiple groups were assessed by a one-way or two-way ANOVA with Tukey's multiple comparison tests. A P value < 0.05 was considered significant. All data are presented as mean ± standard error of the mean (SEM).

Results

IL-10 is mainly produced by myeloid cells in the mouse aorta

To investigate IL-10 expression in immune cells in atherosclerosis, we crossed the VertX IL-10 reporter mice with *Apoe*$^{-/-}$ mice (Fig. 1A). GFP expression was detectable in aortic CD11b$^+$ myeloid cells by flow cytometry (Fig. 1A). In these mice, GFP intensity is proportional to IL-10 expression [20]. In the aorta of 16-week-old Vert-X *Apoe*$^{-/-}$ mice fed CD or WD for 8 weeks, more than 60% of CD45$^+$ live leukocytes were CD11b$^+$ myeloid cells, about 30% were CD19$^+$ B cells, 5% were CD4$^+$ T cells and 5% were (CD19$^+$) CD11b$^+$ B cells (Fig. 1B, and Figure S1).

In the aorta, we found that 15% of all CD4$^+$ T cells, 20% of CD11b$^+$ myeloid cells, and 25% CD11b$^+$ B cells expressed IL-10 (Fig. 1C). A similar pattern was detected in mice challenged with a WD for 8 weeks (Fig. 1D), but the frequencies of IL-10 expressing CD11b$^+$ myeloid cells and CD11b$^+$ B cells were reduced in WD-fed mice (Fig. 1D and Figure S2). No significant changes were detected for CD4$^+$ T cells and B cells (Fig. 1D and Figure S2). These data suggest that CD4$^+$T cells, CD11b$^+$myeloid cells and CD11b$^+$ B cells express IL-10 in the aorta. Because myeloid cells are the most abundant cells in the atherosclerotic aorta (Fig. 1B), myeloid cells may be the most relevant producers of IL-10.

We further analyzed the cellular origin of IL-10 in other organs including spleen, peritoneal lavage fluid and lymph nodes (LNs). Most splenocytes (70%) are B cells, 25% are CD4$^+$ T cells, and the remaining 5% include few CD11b$^+$ myeloid cells and CD11b$^+$ B cells (Fig. 1E). In the spleen, the highest relative proportion of IL-10 expressing cells was found among the CD11b$^+$ myeloid cells, followed by CD4$^+$ T cells, while only few B cells were IL-10 positive (Fig. 1F). Similar results were found in WD-fed mice (Fig. 1G). The proportion of IL-10$^+$ expressing cells among CD11b$^+$ myeloid cells was reduced in mice on WD compared to mice on CD, but still remained the highest, followed by CD4$^+$ T cells and B cells (Fig. 1G).

IL-10-expressing cells were also analyzed in peritoneal lavage fluid (Fig. 1H–J) and in lymph nodes [LNs, (Fig. 1K, M)]. In peritoneal lavage fluid, CD11b$^+$ B cells represented the largest population, followed by B cells and CD4$^+$ T cells (Fig. 1H). No significant IL-10 expression was detected (Fig. 1I, J). LNs contain low numbers of CD11b$^+$ myeloid cells (Fig. 1K). Similar to the spleen, we found that almost 10% of CD11b$^+$ myeloid cells were IL-10$^+$, higher than the proportion in other cell populations analyzed in LNs from both CD and WD fed mice (Fig. 1L, M). Bone marrow cell precursors were also tested, but no relevant IL-10 expression was detected (data not shown). Taken together, these data suggest that IL-10-expressing myeloid cells are a significant source of IL-10 in atherosclerotic mice especially in aorta (Fig. 1).

Resident and inflammatory macrophages are the highest IL-10 producers in the aorta

Macrophages identified by the expression of the F4/80 marker represent 60 to 80% of CD11b$^+$ myeloid cells in aorta (data not shown). We initially studied *Il10* gene expression among all five identified macrophage subsets in mouse atherosclerotic aorta from a previous single-cell RNA sequencing study 4 (Fig. 2A). We found that three

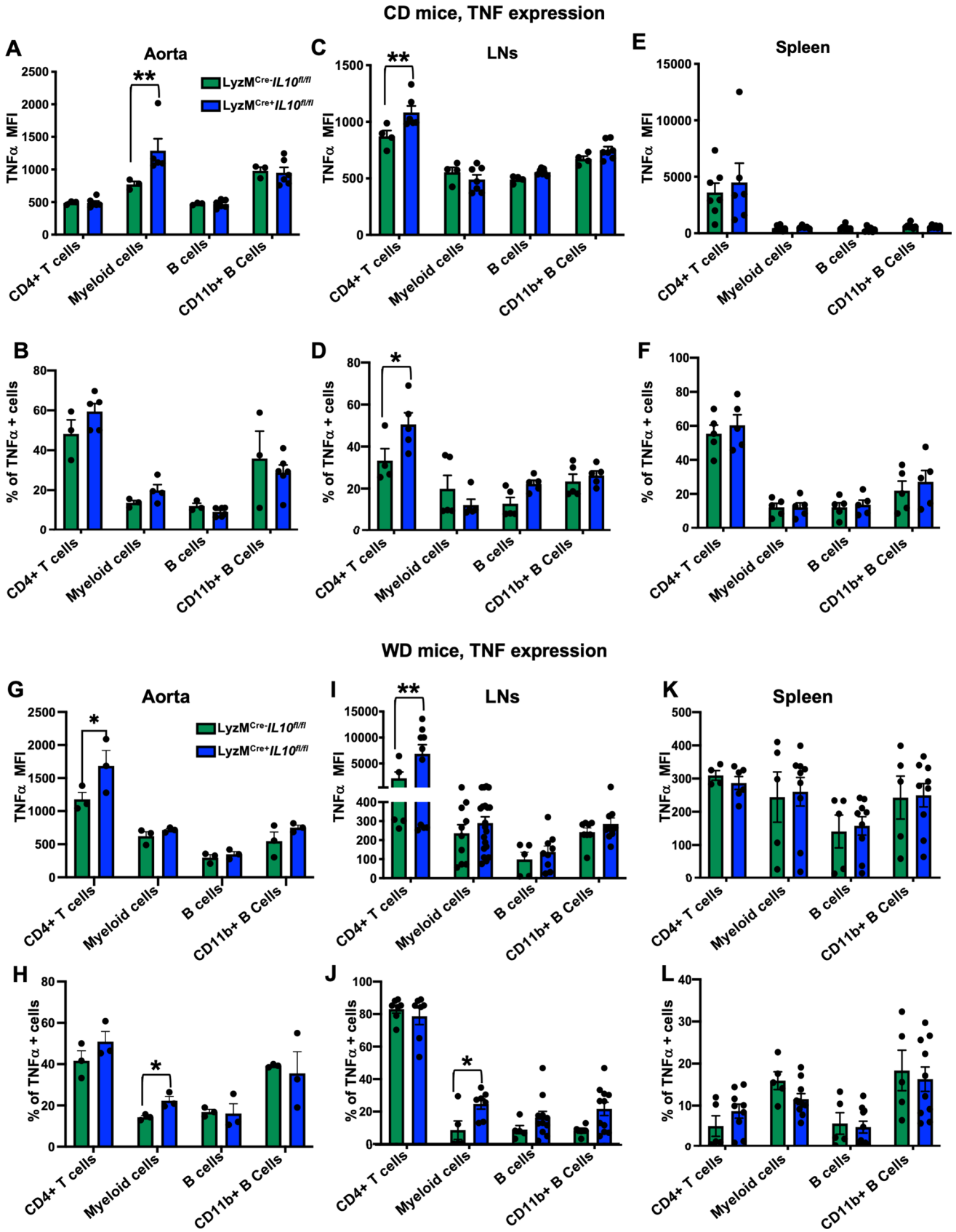
CD mice, TNF expression
A
Aorta
LyzM^Cre-IL10^fl/fl
LyzM^Cre+IL10^fl/fl
TNFα MFI
C
LNs
E
Spleen
B
% of TNFα + cells
D
F
WD mice, TNF expression
G
Aorta
I
LNs
K
Spleen
H
J
L
CD4+ T cells
Myeloid cells
B cells
CD11b+ B Cells

◂**Fig. 5** Myeloid IL-10 depletion induces local increases in TNFα secretion. Leukocyte TNFα intracellular staining expressed as MFI or % in (**A**, **B**) Aorta ($n=3$–5), (**C**, **D**) LNs ($n=4$–6), and (**E**, **F**) Spleens ($n=5$–7). Leukocytes were harvested from *LyzM*$^{Cre+}$*Il10*$^{fl/fl}$ *Apoe*$^{-/-}$, or *LyzM*$^{Cre-}$*Il10*$^{fl/fl}$ *Apoe*$^{-/-}$ mice kept on CD for 25 weeks ($n=3$–5)**.** Leukocyte TNFα intracellular staining expressed as MFI or % of (**G**, **H**) Aorta ($n=3$), (**I**, **J**) LNs ($n=6$), and (**K**, **L**) Spleens ($n=5$–10) leukocytes harvested from *LyzM*$^{Cre+}$*Il10*$^{fl/fl}$ *Apoe*$^{-/-}$, or *LyzM*$^{Cre-}$*Il10*$^{fl/fl}$ *Apoe*$^{-/-}$ mice kept on WD for 12 weeks. Data are presented as mean ± SEM. *P* value was calculated by two-way ANOVA with Tukey's correction for multiple comparison.*$p<0.05$, **$p<0.01$, ***$p<0.001$

macrophage subsets specifically expressed *Il10* mRNA, with the highest proportion found in inflammatory macrophages (18%), followed by IFNIC macrophages (15%), and resident macrophages (10%) (Fig. 2B, C). Next, we used the VertX *Apoe*$^{-/-}$ mice to identify IL-10^{GFP} protein expression in myeloid cells in the aorta. F4/80^{+}macrophages expressed more IL-10^{GFP} than F4/80^{-} myeloid cells (Fig. 2D). Among F4/80^{+} macrophages, an average of 20% were IL-10^{+} as detected by flow cytometry (Fig. 2E). Very few F4/80^{-} myeloid cells expressed IL-10^{GFP} (Fig. 2E). We further used the markers CD206 and Lyve1 to discriminate between macrophage subsets in the aorta of VertX *Apoe*$^{-/-}$ mice. Resident like macrophages were defined as CD206^{+}Lyve1 4, 5. CD206^{+}Lyve1^{+} resident-like macrophages showed the highest IL-10 expression among all F4/80^{+} macrophages (Fig. 2F). Among the non-resident CD206^{-}Lyve1^{-} macrophages fewer than 5% were IL-10^{+} (Fig. 2G). IL-10 expression in macrophages was also confirmed by imaging whole mount aortas of Vert-X *Apoe*$^{-/-}$ mice (Fig. 2H). Co-expression analysis showed that IL-10-expressing macrophages were located both in the adventitia and the intima (Fig. 2I). 24% of all intimal macrophages and only 12% of the adventitial macrophages expressed IL-10 (Fig. 2I). A pre-fixed range of IL-10^{GFP} intensity was used to localize IL-10-expressing macrophages.

Myeloid-specific elimination of IL-10 increases atherosclerosis

To test the impact of myeloid-derived IL-10 on atherosclerosis, we crossed *Il10*$^{fl/fl}$ mice with *Apoe*$^{-/-}$ *LyzM*$^{Cre+}$ mice and investigated atherosclerosis at 25 weeks of CD or 12 weeks of WD (accelerated atherosclerosis model). Plasma IL-10 measured by cytokine bead array (CBA) was reduced by ~90% in *LyzM*$^{Cre+}$ *Il10*$^{fl/fl}$ *Apoe*$^{-/-}$ mice on CD (Fig. 3A). On WD IL-10 was not detectable in *LyzM*$^{Cre+}$ *Il10*$^{fl/fl}$ *Apoe*$^{-/-}$ mice (Fig. 3B). These findings suggest that most or all plasma IL-10 is derived from myeloid cells. IL-10 intracellular staining of LN cells confirmed successful IL-10 ablation in CD11b^{+} myeloid cells of *LyzM*$^{Cre+}$ *Il10*$^{fl/fl}$ *Apoe*$^{-/-}$ mice (Figure S3 A, B). By flow cytometry, we found that myeloid IL-10 ablation increased myeloid cells in the aorta; no other cell proportions were affected (Fig. 3C).

Next, we assessed the impact of myeloid IL-10 on atherosclerosis by measuring atherosclerotic lesion sizes *en face* [28]. *LyzM*$^{Cre-}$*Il10*$^{fl/fl}$*Apoe*$^{-/-}$ mice on CD showed less than 0.2% atherosclerotic lesions (Fig. 3D, E). In *LyzM*$^{Cre+}$ *Il10*$^{fl/fl}$ *Apoe*$^{-/-}$ mice, lesion area was 5 times larger ($p<0.01$, Fig. 3D, E). As expected, WD greatly exacerbated atherosclerosis (Fig. 3F) to a 5% atherosclerotic lesion area in *LyzM*$^{Cre-}$*Il10*$^{fl/fl}$*Apoe*$^{-/-}$ mice. Lesion size was significantly further increased in *LyzM*$^{Cre+}$ *Il10*$^{fl/fl}$ *Apoe*$^{-/-}$ mice (Fig. 3F). These data show that myeloid IL-10 has a major atherosclerosis-dampening effect.

Genetic IL-10 deficiency in myeloid cells had no effect on body weight or blood leukocyte counts, but significantly increased total cholesterol levels in blood plasma of mice on CD (Figure S4A–D). However, there was no change in triglycerides, LDL or HDL cholesterols (Figure S4B). Small changes were found in the body weight of *LyzM*$^{Cre+}$ *Il10*$^{fl/fl}$ *Apoe*$^{-/-}$ mice on WD (Figure S4E). Plasma lipid levels and blood leukocyte counts remained unchanged in WD fed mice (Figure S4E-H).

Eliminating myeloid IL-10 increases circulating cytokine and chemokine levels in *Apoe*$^{-/-}$ mice

We next reasoned that the elimination of myeloid IL-10 may have an impact on circulating cytokines. To assess this, we used CBA to screen for known atherosclerosis-associated protein changes in blood plasma [29]. We found CCL2 (also known as MCP-1) to increase significantly in *LyzM*$^{Cre+}$ *Il10*$^{fl/fl}$ *Apoe*$^{-/-}$ mice fed CD (Fig. 4A). Interleukin (IL)-1β and tumor necrosis factor (TNF)α showed a trend towards increase in *LyzM*$^{Cre+}$ *Il10*$^{fl/fl}$ *Apoe*$^{-/-}$ mice compared to controls; however, no significance was reached (Fig. 4B, C). In the mice fed WD for 12 weeks, the elimination of myeloid IL-10 similarly promoted CCL2 secretion. TNFα secretion was also significantly induced in *LyzM*$^{Cre+}$ *Il10*$^{fl/fl}$ *Apoe*$^{-/-}$ mice fed WD. Similarly, as reported for CD-fed mice, IL-1β levels trended upwards in *LyzM*$^{Cre+}$ *Il10*$^{fl/fl}$ *Apoe*$^{-/-}$ mice but did not reach significance (Fig. 4F). Overall, myeloid IL-10 depletion in both CD and WD-fed mice increases the systemic levels of known proinflammatory cytokines resulting in inflammation and atherosclerosis progression.

To further study the effect of the myeloid IL-10 depletion locally, we next analyzed the levels of TNFα, a pivotal cytokine in the inflammatory cascade, TNFα is highly associated with atherosclerosis initiation and progression [30]. Consistent with elevated circulating TNFα levels in *LyzM-Cre*$^{+}$ *Il10*$^{fl/fl}$ *Apoe*$^{-/-}$ mice (Fig. 4C, F), intracellular staining showed augmented TNFα (both MFI and %) in PMA/ionomycin stimulated aortic and LNs cells of *LyzM*$^{Cre+}$*Il10*$^{fl/fl}$

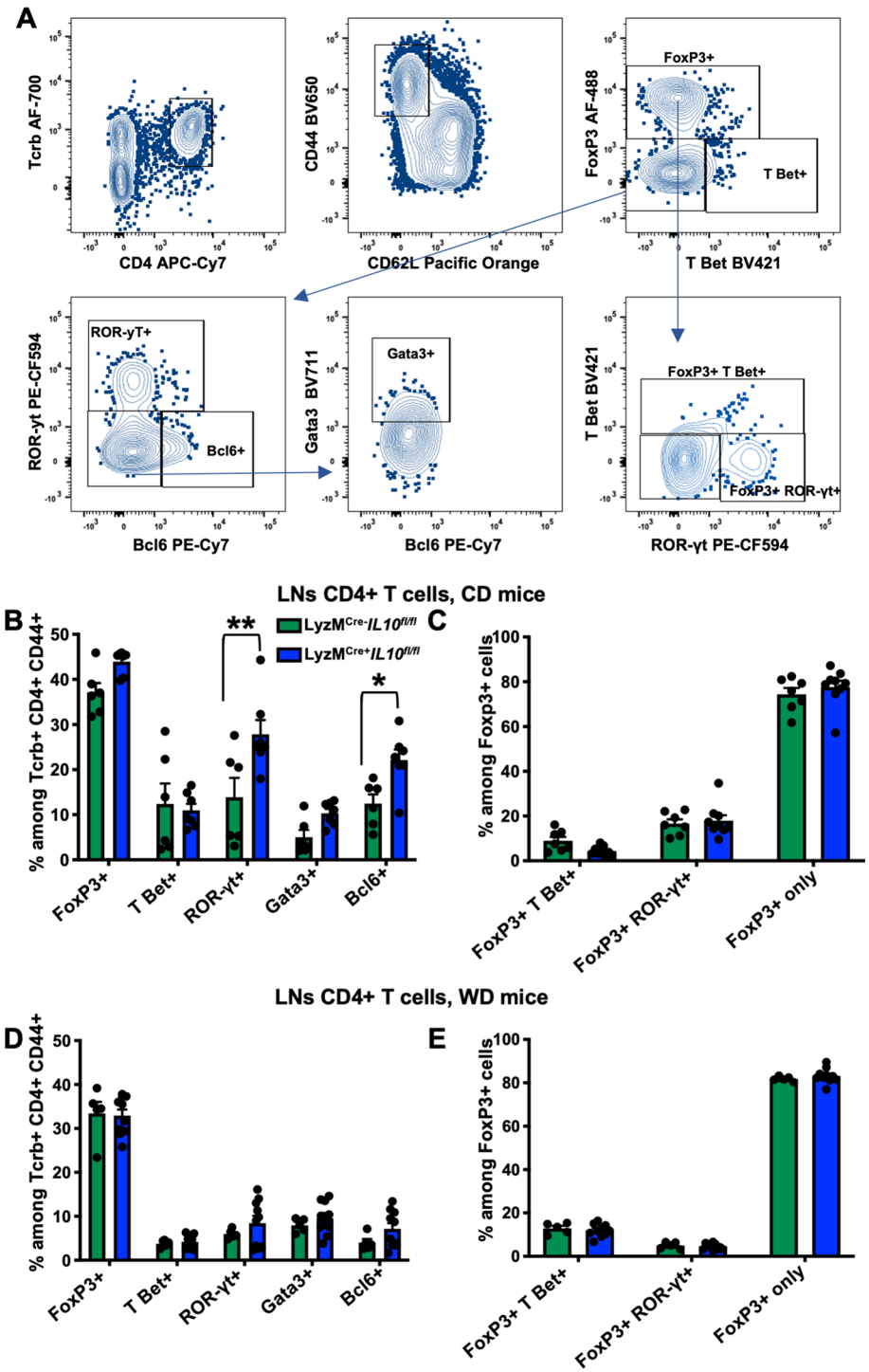

Fig. 6 Myeloid *Il10* deficiency increases frequency of ROR-γt$^+$ Th17 cells in CD but not in WD fed *LyzM*$^{Cre+}$*Il10*$^{fl/fl}$ *Apoe*$^{-/-}$ mice. **A** Applied gating strategy for the identification of the CD4 T cells subpopulations shown as dot plots. **B**–**E** Transcription factors expression among (**B** and **D**) Tcrb$^+$ CD4$^+$ CD44$^+$ CD62L$^-$ T cells or (**C** and **E**) Tcrb$^+$ CD4$^+$ CD44$^+$ CD62L$^-$ FoxP3$^+$ T regs from LNs of *LyzM*$^{Cre+}$*Il10*$^{fl/fl}$ *Apoe*$^{-/-}$ or *LyzM*$^{Cre-}$*Il10*$^{fl/fl}$ *Apoe*.$^{-/-}$ mice fed **B**, **C** CD for 25 weeks ($n=6$) or **D**, **E** WD for 12 weeks ($n=6$–9). Data are presented as mean ± SEM. *P* value was calculated by one-way and two-way ANOVA with Tukey's correction for multiple comparison test $^*p<0.05$, $^{**}p<0.01$

Apoe$^{-/-}$ mice. The largest increase was seen in CD11b$^+$ myeloid cells and CD4$^+$ T cells (Fig. 5A, B and C, D) in aortas and LNs, but not in spleen leukocytes (Fig. 5E and F). In WD fed mice, TNFα MFI was significantly increased in PMA/ionomycin-stimulated aortic and LN CD4$^+$ T cells in *LyzM*$^{Cre+}$*Il10*$^{fl/fl}$ *Apoe*$^{-/-}$ mice (Fig. 5G and H). The proportion of TNFα $^+$ myeloid CD11b$^+$ cells was increased both in aorta and LNs (Fig. 5I and J). No significant changes were found in the spleen (Fig. 5K and L). Thus, we conclude that absence of myeloid IL-10 induces local and systemic increases in TNFα.

IL-10-deficiency in myeloid cells increases ROR-γt$^+$ Th17 cells in CD but not in WD-fed *Apoe*$^{-/-}$ mice

To study the effects of myeloid-derived IL-10, we further analyzed the phenotypic changes in the composition of CD4 T cells in mice fed with CD or WD, known mediators of atherosclerosis progression [31]. We stained draining LNs [32] T cells with monoclonal antibodies to different transcription factors to identify CD4$^+$ T cell Tregs (FoxP3$^+$), Th1 (T-bet$^+$), Th17 (ROR-γt$^+$), Tfh (Bcl6$^+$) and Th2 (GATA-3$^+$) subsets (Fig. 6A). In CD fed *LyzM*$^{Cre+}$ *Il10*$^{fl/fl}$ *Apoe*$^{-/-}$ mice, we found no changes in the frequency of Tregs, Th1, and Th2 subsets compared to *LyzM*$^{Cre-}$*Il10* $^{fl/fl}$*Apoe*$^{-/-}$ mice (Fig. 6B). However, we detected an increased proportion of Th17 and Tfh cells in *LyzM*$^{Cre+}$ *Il10*$^{fl/fl}$ *Apoe*$^{-/-}$ mice (Fig. 6B). The phenotype of Tregs (FoxP3 alone or with TBet or with RORγt) remained unchanged (Fig. 6C). CD4$^+$ T cell subsets including Tregs (FoxP3$^+$), Th1 (T-bet$^+$), Th17 (ROR-γt$^+$), Th2 (GATA-3$^+$) or Tfh (Bcl6$^+$) cells were not affected by myeloid IL-10 deficiency in WD fed mice (Fig. 6D). Most Tregs expressed FoxP3 alone, with some co-expressing T-bet and few co-expressing ROR-γt. This distribution also remained unchanged in animals with myeloid IL-10 deficiency fed WD (Fig. 6E).

Discussion

IL-10 is known to be a potent down-regulator of several cellular processes important in atherosclerosis and plaque development [33]. Thus, IL-10 modulation has been investigated as a possible therapeutic strategy in experimental atherosclerosis [12, 15–17]. This cytokine is known to be produced by several leukocytes, most notably macrophages [34].

Vaccination strategies with peptide epitopes found in ApoB, the main core protein of low-density lipoprotein (LDL) and chylomicrons showed that *Apoe*$^{-/-}$ mice are protected from atherosclerosis when vaccinated [35–38]. In such vaccination experiments, *Il10* mRNA expression was found to be increased in the aortas [35] and in some CD4 T cells [36]. However, the cellular origin of IL-10 during natural atherosclerosis progression or after vaccination was unknown.

In this manuscript, we defined the cellular origin of IL-10 in aortas and other organs of atherosclerotic *Apoe*$^{-/-}$ mice. We found that myeloid cells are a significant source of IL-10 in the aorta in both CD and WD fed mice. CD11b$^+$ B cells also showed IL-10 expression in the aorta. The potential role of B cell–derived IL-10 in atherosclerosis has already been explored. B cell-specific IL-10 depletion showed no effect on atherosclerosis progression [39].

Beyond the local myeloid IL-10, global plasma IL-10 levels were significantly reduced in *LyzM*$^{Cre+}$*Il10*$^{fl/fl}$ *Apoe*$^{-/-}$ mice. Among myeloid populations we focused on macrophages that account for most of the aortic CD11b$^+$ cells. By scRNA-seq data analysis we found that resident and inflammatory macrophages in the aorta expressed *Il10* mRNA, with the inflammatory subsets being the highest. At the protein level, however, we found that CD206$^+$Lyve1$^+$ resident macrophages in the aorta of atherosclerotic *Apoe*$^{-/-}$ mice produced more IL-10 than other immune cells. It is known that the correlation between mRNA and protein expression is limited in immune cells [40].

Through colocalization analysis in whole mount aortas of VertX *Apoe*$^{-/-}$ mice, we further discovered that IL10-expressing macrophages can be located both in the adventitia and the neointima. To directly study the impact of myeloid IL-10 in atherosclerosis progression, we used *LyzM*$^{Cre+}$ *Il10*$^{fl/fl}$ *Apoe*$^{-/-}$ mice. The *LyzM*$^{Cre+}$ targets monocytes, macrophages and neutrophils [21]. However, neutrophils content in the mouse aorta is negligible.

Myeloid IL-10-deficiency boosted myeloid cell proportion in aorta. Similarly, *en face* aortic lesions increased 5-fold and 1.5-fold on CD and WD fed *LyzM*-$^{Cre+}$ *Il10*$^{fl/fl}$ *Apoe*$^{-/-}$ mice, respectively, compared to *LyzM*$^{Cre-}$*Il10*$^{fl/fl}$*Apoe*$^{-/-}$ littermate controls. Plasma lipids levels did not change in myeloid IL-10 depleted WD fed mice. Some variation has been found in the total cholesterols of myeloid IL-10 depleted CD fed mice, no changes in triglyceride or LDL and HDL levels were detected.

These data demonstrate the atheroprotective effects of myeloid cell-derived IL-10, which accounts for most of the secreted IL-10 in *Apoe*$^{-/-}$ mice.

In a previous report, Han X et al. built a lentiviral mediated IL-10 macrophages overexpression model [18]. As expected, they found decreased atherosclerotic lesions in transduced mice further suggesting possible IL-10 autocrine function on macrophages, with increased cholesterol influx and decreased apoptosis. The autocrine function was, however, challenged by a recent report showing that the loss of myeloid IL-10R1 signaling in *Ldlr*$^{-/-}$ mice attenuated atherosclerotic lesion size and severity by modifying the susceptibility to hypercholesterolemia [19]. Thus, this study suggests that the autocrine function of IL-10 likely limits its production in a negative feedback loop.

Furthermore, Han X et al. did not address the myeloid IL-10 production in the normal progression of the disease and did not take into consideration any other possible IL-10 source [18].

We detected increased CCL2 chemokine plasma levels in *LyzM*$^{Cre+}$*Il10*$^{fl/fl}$ *Apoe*$^{-/-}$ mice fed CD and WD. CCL2 has been strongly linked to atherosclerosis in both animal and human studies [41]. CCL2 and its receptor CCR2 are known to regulate and promote the recruitment of classical

monocytes into the atherosclerotic plaque. In humans, increased CCL2 plasma levels have been associated with heart failure and its severity [42].

IL-1β and TNFα are also modulated in plasma of mice lacking myeloid-derived IL-10 on both CD and WD. Both cytokines have been considered among the most important factors promoting inflammatory processes in atherosclerosis [29].

IL-1β is induced in monocytes and macrophages by the activation of the Inflammasome machinery [43, 44] and is known to promote (among other functions) CCL2 expression and recruitment of monocytes and other immune cells [45]. Recently, the CANTOS (Canakinumab Anti-inflammatory Thrombosis Outcome Study) confirmed the importance of IL–1β as therapeutic target for the possible treatment of human atherosclerosis and its complications [46].

TNFα is a member of the TNF superfamily. After binding to its receptors TNFR1 (p55) and TNFR2 (p75), it mediates several proinflammatory functions [47]. In humans, TNF is known to promote the interaction between circulating leukocytes and the endothelium, thus promoting leukocyte recruitment into the atherosclerotic plaque [29]. TNFα was found modulated both systemically and locally as detected by CBA and flow cytometry in both CD and WD-fed $LyzM^{Cre+}Il10^{fl/fl}$ $Apoe^{-/-}$ mice. As expected, WD fed mice showed the strongest and most significant increase. Our data also suggest that local production of TNFα was mostly by $CD11b^+$ myeloid cells and $CD4^+$ T cells in aorta and LNs of mice lacking myeloid IL-10 production.

Phenotypic analysis of common $CD4^+$ T cells also suggests that the depletion of myeloid-derived IL-10 increased ROR-γt^+ Th17 $CD4^+$ T cells in LNs. $LyzM^{Cre+}Il10^{fl/fl}$ $Apoe^{-/-}$ mice fed a WD for 12 weeks did not show increased ROR-γt^+ Th17 $CD4^+$ T cells in LNs compared to $LyzM^{Cre-}Il10^{fl/fl}Apoe^{-/-}$ mice.

Conclusions

In summary, here we show that myeloid cells are the most significant source of IL-10 during atherosclerosis progression in both CD and WD models. The specific loss of myeloid-derived IL-10 promotes a strong proinflammatory state, with increased expression of CCL2, IL-1β and TNFα possibly resulting in the increased recruitment of immune cells, such as T cells and monocyte-derived macrophages, into the atherosclerotic aorta, with the net effect of exacerbating inflammation and promoting atherosclerosis progression in mice.

Supplementary Information The online version contains supplementary material available at https://doi.org/10.1007/s00018-022-04649-9.

Acknowledgements We thank Jacqueline Miller for initial support with maintaining the mouse colony.

Author contributions M.O., D.W. and K.L. contributed to the study conception and design. Material preparation, data collection and analysis were performed by M.O., D.W., V.S., H.W., K.K., J.M., and W.B.K.. The first draft of the manuscript was written by M.O. and K.L. All authors commented on previous versions of the manuscript. All authors read and approved the final manuscript.

Funding This work was supported by grants to M.O. from the American Heart Association grant (AHA18POST34060251), and grant (CDA 941152) and the Conrad Prebys Foundation Award. D.W. was supported by the Deutsche Forschungsgemeinschaft (WO 1994/1-1) and received funding from the European Research Council (ERC) under the European Union's Horizon 2020 research and innovation program (grant agreement No 853425). H.W. was supported by Deutsche Forschungsgemeinschaft (SFB TRR259 (397484323) and CCRC GRK2407 (360043781 to HW)). K.L. was supported by grant P01 HL136275. The Zeiss LSM 880 confocal microscope was funded by NIH S10OD021831.

Data availability All data and methods used in the analysis and materials used to conduct the research will be made available to any researcher for the purpose of reproducing the results or replicating the procedures. All data, methods, and materials are available on personal request at the La Jolla Institute for Immunology, CA.

Declarations

Conflict of interest On behalf of all authors, the corresponding author states that there is no conflict of interest.

Ethical approval All in vivo experiments followed guidelines of the La Jolla Institute for Immunology (LJI) Animal Care and Use Committee. Approval for use of rodents was obtained from LJI according to criteria outlined in the Guide for the Care and Use of Laboratory Animals from the National Institutes of Health.

References

1. Libby P (2021) The changing landscape of atherosclerosis. Nature 592:524–533
2. Roy P, Orecchioni M, Ley K (2021) How the immune system shapes atherosclerosis: roles of innate and adaptive immunity. Nat Rev Immunol 22:251–265
3. Tabas I, Lichtman AH (2017) Monocyte-Macrophages and T Cells in atherosclerosis. Immunity 47:621–634
4. Zernecke A, Winkels H, Cochain C, Williams JW, Wolf D, Soehnlein O, Robbins CS, Monaco C, Park I, McNamara CA, Binder CJ, Cybulsky MI, Scipione CA, Hedrick CC, Galkina EV, Kyaw T, Ghosheh Y, Dinh HQ, Ley K (2020) Meta-analysis of leukocyte diversity in atherosclerotic mouse aortas. Circ Res 127:402–426
5. Lim HY, Lim SY, Tan CK, Thiam CH, Goh CC, Carbajo D, Chew SHS, See P, Chakarov S, Wang XN, Lim LH, Johnson LA, Lum J, Fong CY, Bongso A, Biswas A, Goh C, Evrard M, Yeo KP, Basu R, Wang JK, Tan Y, Jain R, Tikoo S, Choong C, Weninger W, Poidinger M, Stanley RE, Collin M, Tan NS, Ng LG, Jackson DG, Ginhoux F, Angeli V (2018) Hyaluronan receptor LYVE-1-expressing macrophages maintain arterial tone through hyaluronan-mediated regulation of smooth muscle cell collagen. Immunity 49:326–341 (**e7**)
6. Koltsova EK, Hedrick CC, Ley K (2013) Myeloid cells in atherosclerosis: a delicate balance of anti-inflammatory and proinflammatory mechanisms. Curr Opin Lipidol 24:371–380

7. Saraiva M, Vieira P, O'Garra A (2020) Biology and therapeutic potential of interleukin-10. J Exp Med 217(1):e20190418
8. Moore KW, de Waal Malefyt R, Coffman RL, O'Garra A (2001) Interleukin-10 and the interleukin-10 receptor. Annu Rev Immunol 19:683–765
9. Wolk K, Kunz S, Asadullah K, Sabat R (2002) Cutting edge: immune cells as sources and targets of the IL-10 family members? J Immunol 168:5397–5402
10. Mosser DM, Zhang X (2008) Interleukin-10: new perspectives on an old cytokine. Immunol Rev 226:205–218
11. Hutchins AP, Diez D, Miranda-Saavedra D (2013) The IL-10/STAT3-mediated anti-inflammatory response: recent developments and future challenges. Brief Funct Genomics 12:489–498
12. Mallat Z, Besnard S, Duriez M, Deleuze V, Emmanuel F, Bureau MF, Soubrier F, Esposito B, Duez H, Fievet C, Staels B, Duverger N, Scherman D, Tedgui A (1999) Protective role of interleukin-10 in atherosclerosis. Circ Res 85:e17-24
13. Pinderski LJ, Fischbein MP, Subbanagounder G, Fishbein MC, Kubo N, Cheroutre H, Curtiss LK, Berliner JA, Boisvert WA (2002) Overexpression of interleukin-10 by activated T lymphocytes inhibits atherosclerosis in LDL receptor-deficient Mice by altering lymphocyte and macrophage phenotypes. Circ Res 90:1064–1071
14. Pinderski Oslund LJ, Hedrick CC, Olvera T, Hagenbaugh A, Territo M, Berliner JA, Fyfe AI (1999) Interleukin-10 blocks atherosclerotic events in vitro and in vivo. Arterioscler Thromb Vasc Biol 19:2847–2853
15. Potteaux S, Esposito B, van Oostrom O, Brun V, Ardouin P, Groux H, Tedgui A, Mallat Z (2004) Leukocyte-derived interleukin 10 is required for protection against atherosclerosis in low-density lipoprotein receptor knockout mice. Arterioscler Thromb Vasc Biol 24:1474–1478
16. Caligiuri G, Rudling M, Ollivier V, Jacob MP, Michel JB, Hansson GK, Nicoletti A (2003) Interleukin-10 deficiency increases atherosclerosis, thrombosis, and low-density lipoproteins in apolipoprotein E knockout mice. Mol Med 9:10–17
17. Pinderski LJ, Fischbein MP, Subbanagounder G, Fishbein MC, Kubo N, Cheroutre H, Curtiss LK, Berliner JA, Boisvert WA (2002) Overexpression of interleukin-10 by activated T lymphocytes inhibits atherosclerosis in LDL receptor-deficient Mice by altering lymphocyte and macrophage phenotypes. Circ Res 90:1064–1071
18. Han X, Kitamoto S, Wang H, Boisvert WA (2010) Interleukin-10 overexpression in macrophages suppresses atherosclerosis in hyperlipidemic mice. FASEB J 24:2869–2880
19. Stoger JL, Boshuizen MC, Brufau G, Gijbels MJ, Wolfs IM, van der Velden S, Pottgens CC, Vergouwe MN, Wijnands E, Beckers L, Goossens P, Kerksiek A, Havinga R, Muller W, Lutjohann D, Groen AK, de Winther MP (2016) Deleting myeloid IL-10 receptor signalling attenuates atherosclerosis in LDLR$^{-/-}$ mice by altering intestinal cholesterol fluxes. Thromb Haemost 116:565–577
20. Madan R, Demircik F, Surianarayanan S, Allen JL, Divanovic S, Trompette A, Yogev N, Gu Y, Khodoun M, Hildeman D, Boespflug N, Fogolin MB, Grobe L, Greweling M, Finkelman FD, Cardin R, Mohrs M, Muller W, Waisman A, Roers A, Karp CL (2009) Nonredundant roles for B cell-derived IL-10 in immune counter-regulation. J Immunol 183:2312–2320
21. Clausen BE, Burkhardt C, Reith W, Renkawitz R, Forster I (1999) Conditional gene targeting in macrophages and granulocytes using LysMcre mice. Transgenic Res 8:265–277
22. Roers A, Siewe L, Strittmatter E, Deckert M, Schluter D, Stenzel W, Gruber AD, Krieg T, Rajewsky K, Muller W (2004) T cell-specific inactivation of the interleukin 10 gene in mice results in enhanced T cell responses but normal innate responses to lipopolysaccharide or skin irritation. J Exp Med 200:1289–1297
23. Getz GS, Reardon CA (2006) Diet and murine atherosclerosis. Arterioscler Thromb Vasc Biol 26:242–249
24. Butcher MJ, Herre M, Ley K, Galkina E (2011) Flow cytometry analysis of immune cells within murine aortas. J Vis Exp 53:e2848
25. Bankhead P, Loughrey MB, Fernandez JA, Dombrowski Y, McArt DG, Dunne PD, McQuaid S, Gray RT, Murray LJ, Coleman HG, James JA, Salto-Tellez M, Hamilton PW (2017) QuPath: open source software for digital pathology image analysis. Sci Rep 7:16878
26. Korsunsky I, Millard N, Fan J, Slowikowski K, Zhang F, Wei K, Baglaenko Y, Brenner M, Loh PR, Raychaudhuri S (2019) Fast, sensitive and accurate integration of single-cell data with harmony. Nat Methods 16:1289–1296
27. Becht E, McInnes L, Healy J, Dutertre CA, Kwok IWH, Ng LG, Ginhoux F, Newell EW (2018) Dimensionality reduction for visualizing single-cell data using UMAP. Nat Biotechnol
28. Daugherty A, Tall AR, Daemen M, Falk E, Fisher EA, Garcia-Cardena G, Lusis AJ, Owens AP 3rd, Rosenfeld ME, Virmani R (2017) T. American Heart Association Council on Arteriosclerosis, B. Vascular, and S. Council on Basic Cardiovascular, recommendation on design, execution, and reporting of animal atherosclerosis studies: a scientific statement from the American Heart Association. Arterioscler Thromb Vasc Biol 37:e131–e157
29. Tousoulis D, Oikonomou E, Economou EK, Crea F, Kaski JC (2016) Inflammatory cytokines in atherosclerosis: current therapeutic approaches. Eur Heart J 37:1723–1732
30. McKellar GE, McCarey DW, Sattar N, McInnes IB (2009) Role for TNF in atherosclerosis? Lessons from autoimmune disease. Nat Rev Cardiol 6:410–417
31. Winkels H, Wolf D (2021) Heterogeneity of T cells in atherosclerosis defined by single-cell RNA-sequencing and cytometry by time of flight. Arterioscler Thromb Vasc Biol 41:549–563
32. Wolf D, Ley K (2019) Immunity and Inflammation in atherosclerosis. Circ Res 124:315–327
33. Mallat Z, Heymes C, Ohan J, Faggin E, Leseche G, Tedgui A (1999) Expression of interleukin-10 in advanced human atherosclerotic plaques: relation to inducible nitric oxide synthase expression and cell death. Arterioscler Thromb Vasc Biol 19:611–616
34. Kleemann R, Zadelaar S, Kooistra T (2008) Cytokines and atherosclerosis: a comprehensive review of studies in mice. Cardiovasc Res 79:360–376
35. Tse K, Gonen A, Sidney J, Ouyang H, Witztum JL, Sette A, Tse H, Ley K (2013) Atheroprotective vaccination with MHC-II restricted peptides from ApoB-100. Front Immunol 4:493
36. Kimura T, Tse K, McArdle S, Gerhardt T, Miller J, Mikulski Z, Sidney J, Sette A, Wolf D, Ley K (2017) Atheroprotective vaccination with MHC-II-restricted ApoB peptides induces peritoneal IL-10-producing CD4 T cells. Am J Physiol Heart Circ Physiol 312:H781–H790
37. Kimura T, Kobiyama K, Winkels H, Tse K, Miller J, Vassallo M, Wolf D, Ryden C, Orecchioni M, Dileepan T, Jenkins MK, James EA, Kwok WW, Hanna DB, Kaplan RC, Strickler HD, Durkin HG, Kassaye SG, Karim R, Tien PC, Landay AL, Gange SJ, Sidney J, Sette A, Ley K (2018) Regulatory CD4(+) T cells recognize MHC-II-restricted peptide epitopes of apolipoprotein B. Circulation 138:1130–1143
38. Kobiyama K, Vassallo M, Mitzi J, Winkels H, Pei H, Kimura T, Miller J, Wolf D, Ley K (2018) A clinically applicable adjuvant for an atherosclerosis vaccine in mice. Eur J Immunol 48:1580–1587
39. Sage AP, Nus M, Baker LL, Finigan AJ, Masters LM, Mallat Z (2015) Regulatory B cell-specific interleukin-10 is dispensable for atherosclerosis development in mice. Arterioscler Thromb Vasc Biol 35:1770–1773

40. Koussounadis A, Langdon SP, Um IH, Harrison DJ, Smith VA (2015) Relationship between differentially expressed mRNA and mRNA-protein correlations in a xenograft model system. Sci Rep 5:10775
41. Noels H, Weber C, Koenen RR (2019) Chemokines as therapeutic targets in cardiovascular disease. Arterioscler Thromb Vasc Biol 39:583–592
42. Hage C, Michaelsson E, Linde C, Donal E, Daubert JC, Gan LM, Lund LH (2017) Inflammatory biomarkers predict heart failure severity and prognosis in patients with heart failure with preserved ejection fraction: a holistic proteomic approach. Circ Cardiovasc Genet 10:e001633
43. Martinon F, Burns K, Tschopp J (2002) The inflammasome: a molecular platform triggering activation of inflammatory caspases and processing of proIL-beta. Mol Cell 10:417–426
44. Karasawa T, Takahashi M (2017) Role of NLRP3 inflammasomes in atherosclerosis. J Atheroscler Thromb 24:443–451
45. Kirii H, Niwa T, Yamada Y, Wada H, Saito K, Iwakura Y, Asano M, Moriwaki H, Seishima M (2003) Lack of interleukin-1beta decreases the severity of atherosclerosis in ApoE-deficient mice. Arterioscler Thromb Vasc Biol 23:656–660
46. Ridker PM, Everett BM, Thuren T, MacFadyen JG, Chang WH, Ballantyne C, Fonseca F, Nicolau J, Koenig W, Anker SD, Kastelein JJP, Cornel JH, Pais P, Pella D, Genest J, Cifkova R, Lorenzatti A, Forster T, Kobalava Z, Vida-Simiti L, Flather M, Shimokawa H, Ogawa H, Dellborg M, Rossi PRF, Troquay RPT, Libby P, Glynn RJ, C.T. Group (2017) Antiinflammatory therapy with canakinumab for atherosclerotic disease. N Engl J Med 377:1119–1131
47. Parameswaran N, Patial S (2010) Tumor necrosis factor-alpha signaling in macrophages. Crit Rev Eukaryot Gene Expr 20:87–103

Publisher's Note Springer Nature remains neutral with regard to jurisdictional claims in published maps and institutional affiliations.

Springer Nature or its licensor (e.g. a society or other partner) holds exclusive rights to this article under a publishing agreement with the author(s) or other rightsholder(s); author self-archiving of the accepted manuscript version of this article is solely governed by the terms of such publishing agreement and applicable law.